



## 光学势灵敏区域的能量相依性研究

杨磊 林承键 贾会明 王东玺 杨峰 钟福鹏 钟善豪 马南茹 温培威

### Energy Dependence of the Radial Sensitivity

YANG Lei, LIN Chengjian, JIA Huiming, WANG Dongxi, YANG Feng, ZHONG Fupeng, ZHONG Shanhao, MA Nanru, WEN Peiwei

在线阅读 View online: <https://doi.org/10.11804/NuclPhysRev.37.2019CNPC25>

#### 引用格式:

杨磊, 林承键, 贾会明, 王东玺, 杨峰, 钟福鹏, 钟善豪, 马南茹, 温培威. 光学势灵敏区域的能量相依性研究[J]. *原子核物理评论*, 2020, 37(3):595–599. doi: 10.11804/NuclPhysRev.37.2019CNPC25

YANG Lei, LIN Chengjian, JIA Huiming, WANG Dongxi, YANG Feng, ZHONG Fupeng, ZHONG Shanhao, MA Nanru, WEN Peiwei. Energy Dependence of the Radial Sensitivity[J]. *Nuclear Physics Review*, 2020, 37(3):595–599. doi: 10.11804/NuclPhysRev.37.2019CNPC25

## 您可能感兴趣的其他文章

### Articles you may be interested in

#### 弱束缚原子核引起的熔合反应机制研究

Study of Fusion Reaction Mechanism Induced by Weakly Bound Nuclei

原子核物理评论. 2020, 37(2): 119–135 <https://doi.org/10.11804/NuclPhysRev.37.2019060>

#### 基于折叠势的两势方法系统研究质子放射性(英文)

Systematic Study of Proton Radioactivity Based on Two-potential Approach with Folding Potentials

原子核物理评论. 2018, 35(3): 257–263 <https://doi.org/10.11804/NuclPhysRev.35.03.257>

#### 原子核放射性对核对称能的约束 (英文)

Nuclear Symmetry Energy Constrained by Nuclear Radioactivities

原子核物理评论. 2017, 34(1): 46–50 <https://doi.org/10.11804/NuclPhysRev.34.01.046>

#### $\Delta$ 共振态的硬过程及软过程产生截面在同位旋不对称核体系下的介质修正研究

Study of Medium Modifications on  $\Delta$  Production Cross Sections of both Hard and Soft Processes from the Isospin Asymmetric Nuclear System

原子核物理评论. 2018, 35(4): 374–381 <https://doi.org/10.11804/NuclPhysRev.35.04.374>

#### 中能重离子碰撞中横向流电荷依赖的形状以及实验条件对横向流的影响(英文)

Z-dependence Flow Pattern and Experimental Filter Effect on Transverse Flow Extraction in Intermediate-energy Heavy Ion Collisions

原子核物理评论. 2018, 35(1): 18–22 <https://doi.org/10.11804/NuclPhysRev.35.01.018>

#### 140 AMeV $^{58,64}\text{Ni}+^9\text{Be}$ 反应中同位旋标度规律的研究

Study of the Nuclear Matter Symmetry Energy in the Simulated 140 AMeV  $^{58,64}\text{Ni}+^9\text{Be}$  Reactions by Isoscaling Method

原子核物理评论. 2017, 34(3): 525–528 <https://doi.org/10.11804/NuclPhysRev.34.03.525>

Article ID: 1007-4627(2020)03-0595-05

## Energy Dependence of the Radial Sensitivity

YANG Lei, LIN Chengjian<sup>†</sup>, JIA Huiming, WANG Dongxi, YANG Feng,  
ZHONG Fupeng, ZHONG Shanhao, MA Nanru, WEN Peiwei

(China Institute of Atomic Energy, Beijing 102413, China)

**Abstract:** With the application of the notch technique, the radial sensitive regions for the tightly bound system  $^{16}\text{O}+^{208}\text{Pb}$ , and weakly bound system  $^9\text{Be}+^{208}\text{Pb}$  were investigated. It is the first time that the shape and resonant scattering can be identified from the sensitivity functions. Moreover, strong energy dependence of sensitive regions were found for both the tightly and stable weakly bound systems: in the above barrier region, the sensitive region varies around the strong absorption radius; while below the barrier, the behavior of sensitive region is close to that of the closest approach in the Coulomb field.

**Key words:** optical model potential; sensitive region; energy dependence; tightly bound nuclear system; weakly bound nuclear system

CLC number: O532.33

Document code: A

DOI: 10.11804/NuclPhysRev.37.2019CNPC25

### 1 Introduction

Although elastic scattering is the simplest interaction process in the collision of two nuclei, it is the primary source of the information on the nuclear potential. With the long-term and systematic studies, some basic properties of the optical model potential (OMP) of heavy-ion reaction systems have been recognized, *e.g.*, the threshold anomaly (TA), which was first observed in the scattering of  $^{16}\text{O}+^{208}\text{Pb}$ <sup>[1]</sup> and refers to the energy dependence of the real and imaginary parts of OMP in the region around the Coulomb barrier. TA is characterized by the sharp decrease of the imaginary part of the potential as the bombarding energy decreases towards the Coulomb barrier, associated with a localized peak around the barrier in the real part. The dispersion relation<sup>[2]</sup>, which arises from the causality principle, can be adopted to describe the connection between the real and imaginary potentials. The situation, however, is more complicated for the systems involving weakly bound nuclei, such as  $^6\text{Li}$ <sup>[3]</sup>,  $^6\text{He}$ <sup>[4-7]</sup> and  $^9\text{Be}$ <sup>[8]</sup>. In these systems, a distinct manifestation of the OMP is observed, demonstrated as an increasing trend in the imaginary potential with energy decreasing below the barrier. Moreover, the application of the dispersion re-

lation is still deserved a further investigation<sup>[6]</sup>.

Since the OMP can be determined unambiguously only at the sensitive radius, it is crucial and necessary to investigate what radial regions of the nuclear potential can be well mapped before we make any discussions on the properties of OMP. The frequently used method to determine the sensitive region (SR) is to find the crossing-point radius of the potential<sup>[9-10]</sup>. However, such a sharply-defined sensitive radius is incompatible with the principles of quantum mechanics, and its value varies with different radial form factors adopted for the OMP<sup>[11]</sup>. As an alternative, the notch technique, which permits an intuitionistic investigation of SR, has been developed by Cramer *et al.*<sup>[12]</sup>. In the previous work<sup>[13]</sup>, the sensitivities of the notch technique on the perturbation parameters, as well as the experimental data have been investigated in detail. Based on the results, in the present work, the notch method is further applied to study the qualities of the SR of the tightly ( $^{16}\text{O}+^{208}\text{Pb}$ ) and weakly bound ( $^9\text{Be}+^{208}\text{Pb}$ ) scattering systems, within the energy region near and above the Coulomb barrier.

### 2 Data analysis

The principle of the notch technique is to intro-

Received date: 28 Dec. 2019; Revised date: 20 Mar. 2020

Foundation item: National Key R&D Program of China(2018YFA0404404); National Natural Science Foundation of China(11635015, U1732145, 11705285, U1867212, 11805280, 11961131012); Continuous Basic Scientific Research Project(WDJC-2019-13)

Biography: YANG Lei(1985-), male, Weihai, Shandong, associate researcher, working on the experimental nuclear physics

<sup>†</sup> Corresponding author: LIN Chengjian, E-mail: cjlin@ciae.ac.cn.

duce a localized perturbation into either the real or imaginary radial potential, and move the notch radially through the potential to investigate the influence arising from this perturbation on the predicted cross section<sup>[12]</sup>.

The nuclear potential is defined as

$$U_N = V(r) + iW(r) = -V_0 f_V(r) - iW_0 f_W(r), \quad (1)$$

where the  $V_0$  and  $W_0$  are depths of the real and imaginary parts of the potential with Woods-Saxon form  $f_i(r, a, R)$ ,

$$f_i(r, a, R) = \left[ 1 + \exp\left(\frac{r - R_i}{a_i}\right) \right]^{-1}, i = V, W, \quad (2)$$

where  $R_i = r_{0i}(A_p^{1/3} + A_T^{1/3})$ , and  $A_p$  and  $A_T$  represent the mass numbers of the projectile and target, respectively.

Taking the real potential  $V(r)$  as an example, the perturbation of the potential  $V_{\text{notch}}$  can be expressed as

$$V_{\text{notch}} = dV_0 f_V(R', a, R) f_{\text{notch}}(r, a', R'), \quad (3)$$

where  $R'$  and  $a'$  represent the position and width of the notch,  $d$  is the fraction by which the potential is reduced, and  $f_{\text{notch}}(r, a', R')$  is the derivative Woods-Saxon surface form factor:

$$f_{\text{notch}}(r, a', R') = \frac{4 \exp\left(\frac{r - R'}{a'}\right)}{\left[ 1 + \exp\left(\frac{r - R'}{a'}\right) \right]^2}. \quad (4)$$

Thus the perturbed real potential  $V(r)_{\text{pert.}}$  is

$$V(r)_{\text{pert.}} = V_0 f_V(r, a, R) - V_{\text{notch}}. \quad (5)$$

The perturbation for the imaginary potential can be derived with the same procedure.

When the perturbation is located in the sensitive region, where the predicted cross section depends strongly on the details of the potential, the calculated elastic scattering angular distribution will change greatly. This means, when compared with the experimental data, there will be a dramatic variation in the  $\chi^2$  value. Conversely, at positions where the evaluated cross section is not sensitive to the potential, the perturbation has little influence on the calculated angular distribution. By means of the notch technique, the sensitive region of the nuclear potential can be presented visually and explicitly.

Based on our pervious work<sup>[13]</sup>, the values of  $d$  and  $a'$  are fixed at 1.0 and 0.05 fm, respectively, with the integration step size  $dr$  kept at 0.01 fm. The Woods-Saxon radial form factor is adopted for the nuclear potential. All the optical model (OM) calculations in the present work are performed with the code

FRESCO<sup>[14]</sup>. The reduced radius  $r_0$  and diffuseness parameter  $a$  of the OMP are fixed at 1.25, 0.65 fm for the  $^{16}\text{O} + ^{208}\text{Pb}$ , and 1.24, 0.63 fm for the  $^9\text{Be} + ^{208}\text{Pb}$ , leaving the depths of the real and imaginary parts to be extracted by fitting the elastic scattering angular distributions.

The radial sensitivities of  $^{16}\text{O} + ^{208}\text{Pb}$  and  $^9\text{Be} + ^{208}\text{Pb}$  at some typical energies are shown in Figs. 1 and 2, respectively. As references, several important radii and distances are labeled in the figures, *e.g.*, the radius of the Coulomb barrier  $R_B$ , the radius of the nuclear potential  $R_{\text{int}}$ , as well as  $D_0$ , at which the nuclear force begins to take effect, defined as where the  $d\sigma_{\text{el}}/d\sigma_{\text{Ru}}$  drops to 0.98 from the unity.

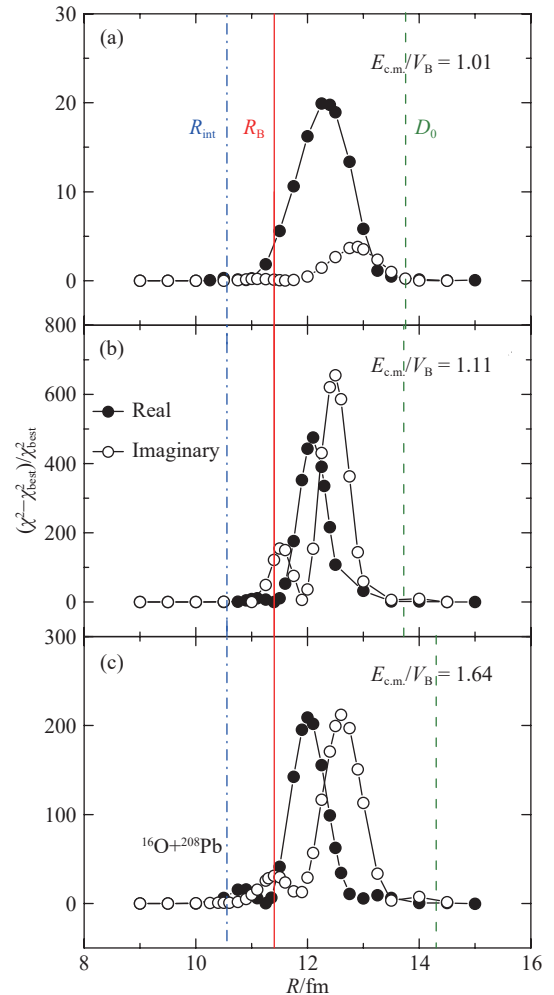


Fig. 1 (color online) The sensitivity functions for the real part (full circle) and imaginary part (hallow circle) potentials for  $^{16}\text{O} + ^{208}\text{Pb}$  at some typical energies. The experimental elastic scattering data are taken from Refs. [15–17]. The height of the Coulomb barrier  $V_B$  is fixed at 73.39 MeV. The vertical solid, dashed, and dash-dotted curves denote the positions of the Coulomb barrier,  $D_0$  and  $R_{\text{int}}$ , respectively. See text for the detail.

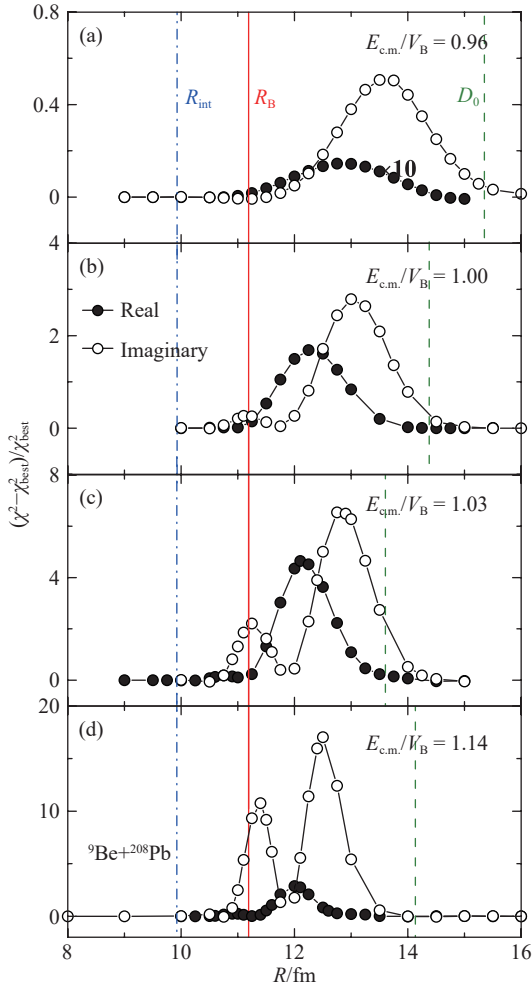


Fig. 2 (color online) Same as Fig. 1, but for the  ${}^9\text{Be}+{}^{208}\text{Pb}$  system, with the experimental data taken from Ref. [8]. The  $V_B$  is fixed at 37.06 MeV.

According to the results, one can find that all the radial SRs locate between the  $R_{\text{int}}$  and  $D_0$ , indicating that the nuclear interior can not be probed by the heavy-ion-heavy-ion elastic scattering at low energies. Meanwhile, SR becomes broader as the bombarding energy decreases, demonstrating that the sensitivity of the experimental data on the details of the nuclear potential turns to be weaker, due to the effect of the Coulomb repulsion. It can be confirmed further by the variations of the relative  $\chi^2$  values, which become larger with the bombarding energy increases.

On the other hand, two distinct peaks are present in both the real and imaginary parts within the above barrier energy region. The amplitude of the inner peak decreases rapidly with the energy going down to the sub-barrier, especially for the real part, the inner peak of which is too small to be recognized in the lower energy region. Moreover, the position of the inner peak almost keeps fixed, having no dependence on the bombarding energy: for the real part, the inner peak lies

inside of  $R_B$ , while that of the imaginary part locates around  $R_B$ . Therefore the inner peak should be responsible to the process of the barrier penetration, *i.e.*, the inner peak of the real part corresponds to the resonance scattering process, and that of the imaginary part is arising from the fusion reaction. With the energy decreasing towards the barrier, the probability of the barrier penetration reduces, leading to the inner peak becomes weak in the lower energy region. The outer peaks, however, locate away from  $R_B$ . Thus they should be mainly responsible for the surface interaction, *i.e.*, the direct interaction process. Moreover, the position of the direct reaction peak of the real part always locates inside, about 0.7 fm, of that of the imaginary part, indicating that the imaginary potential owns a larger SR than that of the real potential.

The energy dependence of the radial SRs (position of the peak) of both the  ${}^{16}\text{O}+{}^{208}\text{Pb}$  and  ${}^9\text{Be}+{}^{208}\text{Pb}$  systems is shown in Fig. 3, where the error bars reflect the width (sigma) of SR. It can be

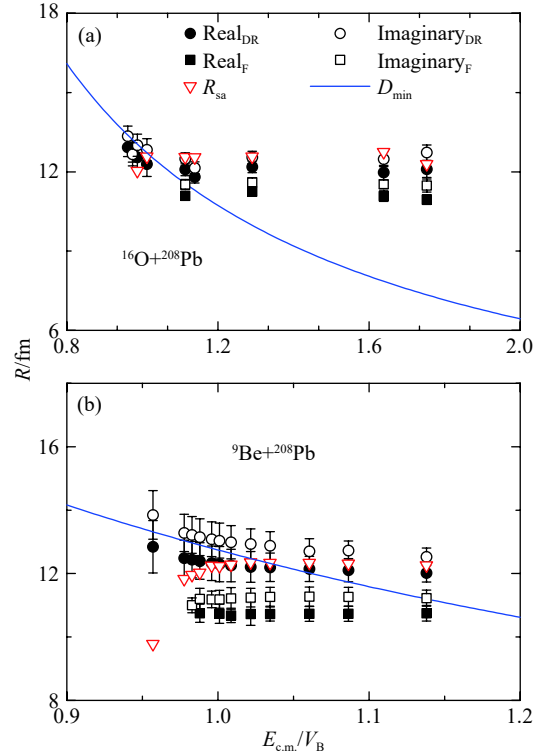


Fig. 3 (color online) Energy dependence of the SRs of (a)  ${}^{16}\text{O}+{}^{208}\text{Pb}$  and (b)  ${}^9\text{Be}+{}^{208}\text{Pb}$ . The full and hollow circles represent results of the surface interaction of the real (real<sub>DR</sub>) and imaginary (imaginary<sub>DR</sub>) parts, respectively. The full and hollow squares denote the inner SRs of the real (real<sub>F</sub>) and imaginary (imaginary<sub>F</sub>) potentials. The triangles are the  $R_{\text{sa}}$  extracted from the experimental data. And the solid curves represent the theoretical  $D_{\text{min}}$ .

seen that in the above barrier region, the positions of the direct interaction peaks ( $SR_{DR}$ ) locates around the strong absorption radius ( $R_{sa}$ ), corresponding to the radius where the observed elastic scattering cross section has fallen to one-fourth of the Rutherford value<sup>[18]</sup>. In the sub-barrier region, however, the variation trend of  $SR_{DR}$  is compatible with closest approach in the Coulomb field  $D_{min}$ , as shown by the solid curve. In the case of head-on collision,  $D_{min}$  is expressed as  $2Z_1Z_2e^2/\mu v_{lab}^2$ , where  $Z_1$  and  $Z_2$  are the charge numbers,  $\mu$  is the reduced mass number,  $v_{lab}$  is the incident velocity in the laboratory frame. Therefore, the energy dependence of the location of  $SR_{DR}$  can be described by a simple expression, as

$$\begin{cases} SR_{DR} = D_{min} & E_{c.m.} < V_B \\ SR_{DR} = R_{sa} & E_{c.m.} \geq V_B \end{cases} \quad (6)$$

The positions of the inner SRs ( $SR_F$ ), which corresponds to the barrier penetration process, locates around the Coulomb barrier, and can be expressed as  $SR_F = R_B$ .

### 3 Conclusion

In summary, the notch technique was applied to study the radial SRs of the tightly and weakly bound systems. The origins of the peaks present in the sensitivity functions are identified: the outer peak corresponds to the surface interaction, while the inner peak is arising from the Coulomb barrier penetration process. Thus, the shape scattering and resonant scattering can be disentangled, and the information of the Coulomb barrier, such as the barrier radius, can be provided. Moreover, the systematic energy dependence of SR were found for both the tightly and stable weakly bound systems: in the above barrier region, SR is equal to  $R_{sa}$ ; while below the barrier, SR can be described by  $D_{min}$ . In consideration of the significance of the energy dependence of SR in the studies of OMP, it is strongly desired to make a further investigation

with the notch technique in a wide range of systems, to obtain a global and universal understanding on the properties of the interaction potentials, especially for the exotic nuclear systems.

### References:

- [1] LILLEY J S, FULTON B R, BANES D, et al. *Phys Lett B*, 1983, 128: 153.
- [2] MAHAX C, NGO H, SATCHLER G R. *Nucl Phys A*, 1986, 449: 354.
- [3] KEELEY N, BENNETT S J, CLARKE N M, et al. *Nucl Phys A*, 1994, 571: 326.
- [4] GARCIA A R, LUBIAN J, PARDRON I, et al. *Phys Rev C*, 2007, 76: 067603.
- [5] YANG L, LIN C J, JIA H M, et al. *Phys Rev C*, 2014, 89: 044615.
- [6] YANG L, LIN C J, JIA H M, et al. *Phys Rev Lett*, 2017, 119: 042503.
- [7] YANG L, LIN C J, JIA H M, et al. *Phys Rev C*, 2017, 96: 044615.
- [8] YU N, ZHUANG H Q, JIA H M, et al. *J Phys G: Nucl Part Phys*, 2010, 37: 075108.
- [9] LIN C J, XU J C, ZHUANG H Q, et al. *Phys Rev C*, 2001, 63: 064606.
- [10] ROUBOS D, PAKOU A, ALAMANOS N, et al. *Phys Rev C*, 2006, 73: 051603.
- [11] MACFARLANE M H, PIEPER S C. *Phys Lett B*, 1981, 103: 169.
- [12] CRAMER J G, DEVRIES R M. *Phys Rev C*, 1980, 22: 91.
- [13] YANG L, LIN C J, JIA H M, et al. *Chin Phys C*, 2016, 40: 056201.
- [14] THOMPSON I J. *Comp Phys Rep*, 1988, 7: 167.
- [15] SILVA C P, ALVAREZ M A G, CHAMON L C, et al. *Nucl Phys A*, 2001, 679: 287.
- [16] PIEPER S C, MACFARLANE M H, GLOECKNER D H, et al. *Phys Rev C*, 1978, 18: 180.
- [17] VIDEBAED F, GOLDSTEIN R B, GRODZINS L, et al. *Phys Rev C*, 1977, 15: 954.
- [18] BASS R. *Nuclear Reactions with Heavy Ion[M]*. New York: SpringerVerlag, 1980.

## 光学势灵敏区域的能量相依性研究

杨磊, 林承键<sup>†</sup>, 贾会明, 王东玺, 杨峰, 钟福鹏, 钟善豪, 马南茹, 温培威

(中国原子能科学研究院, 北京 102413)

**摘要:** 应用扰动法提取和研究了紧束缚体系  $^{16}\text{O}+^{208}\text{Pb}$  和弱束缚体系  $^9\text{Be}+^{208}\text{Pb}$  灵敏区域。首次区分了对应于形状散射和共振散射对应的灵敏区域。同时, 发现紧束缚体系和弱束缚体系的灵敏区域都存在着强烈的能量相依性: 在垒上区域, 灵敏区域在强吸收半径附近变化; 而在垒下能区, 灵敏区域与纯库仑场中的最趋近距离有相似的变化趋势。

**关键词:** 光学势; 灵敏区域; 能量相依性; 紧束缚体系; 弱束缚体系

收稿日期: 2019-12-28; 修改日期: 2020-03-20

基金项目: 国家重点研发计划资助项目 (2018YFA0404404); 国家自然科学基金资助项目 (11635015, U1732145, 11705285, U1867212, 11805280, 11961131012); 财政部基础研究稳定支持项目 (WDJC-2019-13)

<sup>†</sup> 通信作者: 林承键, E-mail: [cjlin@ciae.ac.cn](mailto:cjlin@ciae.ac.cn)。